ELSEVIER

Polymer 42 (2001) 8891–8895

polymer

www.elsevier.com/locate/polymer

Polymer Communication

Irradiation and the glass transition in PEEK

A.S. Vaughan[a,*], G.C. Stevens[b]

[a]*Department of Electronics and Computer Science, ECS, Faraday Building, University of Southampton, Highfield, Southampton SO17 1BJ, UK*
[b]*Polymer Research Centre, University of Surrey, Guildford GU2 7XH, UK*

Received 11 May 2001; received in revised form 5 June 2001; accepted 8 June 2001

Abstract

The influence of electron irradiation on the glass transition temperature, T_g, of poly(ether ether ketone) (PEEK) has been investigated by differential scanning calorimetry, up to a dose of 100 MGy. For amorphous PEEK, the observed T_g increases linearly with absorbed dose at a rate of 0.18°C MGy^{-1}. This indicates the formation of crosslinks, as deduced elsewhere. Above ~50 MGy, these crosslinks prevent crystallization on heating to above T_g, whereas at lower doses, the polymer is able to crystallize to some degree. Qualitatively, the variations in T_g seen in these partially crystalline samples can be explained in terms of a number of factors. The crystals serve to constrain the amorphous fraction, resulting in a direct elevation in T_g. This is reinforced through the rejection of crosslinks from crystalline regions, so resulting in an increase in the local amorphous crosslink density. Conversely, crosslinking can also serve to inhibit crystallization. Quantitatively, models based solely upon the percentage crystallinity are, however, unable to account fully for the variations in T_g that are seen. In contrast, a model based on both overall crystallinity and lamellar thickness gives good agreement with experiment over the complete crystallinity range.

Keywords: Poly(ether ether ketone); Glass transition; Electron irradiation

1. Introduction

The potential of the high performance aromatic polymer poly(ether ether ketone) (PEEK) for use in demanding applications has meant that many aspects of its radiation response have been considered (see for example, Refs. [1–4]). From such work, it is evident that PEEK is highly resistant to ionizing radiation, such as high energy electrons [5,6]. The observed effects have been interpreted in terms of crosslink formation in amorphous regions and progressive destruction of crystallinity [7,8]. Above 15 MGy, gels have been extracted, which can constitute up to 75% by mass of the initial material [8].

The effect of crosslinking on molecular mobility and, hence, the glass transition temperature, has been considered both experimentally and theoretically. Theoretical treatments predict that T_g should increase linearly with crosslink density [9], and such a dependence has been reported for a series of ethylene glycol bis(allylcarbonate)-*co*-allyl ethoxyethyl carbonate [10] and styrene-*co*-divinyl benzene [11] polymer networks, where the crosslink density has been varied by adjusting the chemical composition of the system.

In this short communication, we report on variations in the glass transition temperature seen in a series of PEEK samples, all of which had been subjected to electron irradiation in the amorphous state. In addition to describing the direct effect of the radiation treatment on T_g, we will also consider the consequences of subsequent crystallization.

2. Experimental

The PEEK considered here was obtained from ICI in the form of an amorphous sheet. Gel permeation chromatography resulted in average molecular mass values of $M_w = 4.1 \times 10^4$ and $M_n = 1.3 \times 10^4$, respectively. Samples of this material were wrapped in aluminium foil and irradiated directly using a Van de Graaff electron accelerator operating at 1 MeV and a flux density of 9 μA cm^{-2}. This is equivalent to a dose rate of 1.1 MGy min^{-1} [8]. All irradiations were performed in air upon a water-cooled block, to prevent undue sample heating. Subsequent thermal characterization was carried out using a Perkin–Elmer DSC7 differential scanning calorimeter. All samples were first heated from 50 to 400°C at 10°C min^{-1} (first scan) and, then, rapidly cooled from the melt to 50°C in the calorimeter, whereupon,

* Corresponding author. Tel.: +44-23-8059-3398; fax: +44-23-8059-3709.
E-mail address: asv@ecs.soton.ac.uk (A.S. Vaughan).

0032-3861/01/$ - see front matter
PII: S0032-3861(01)00444-X

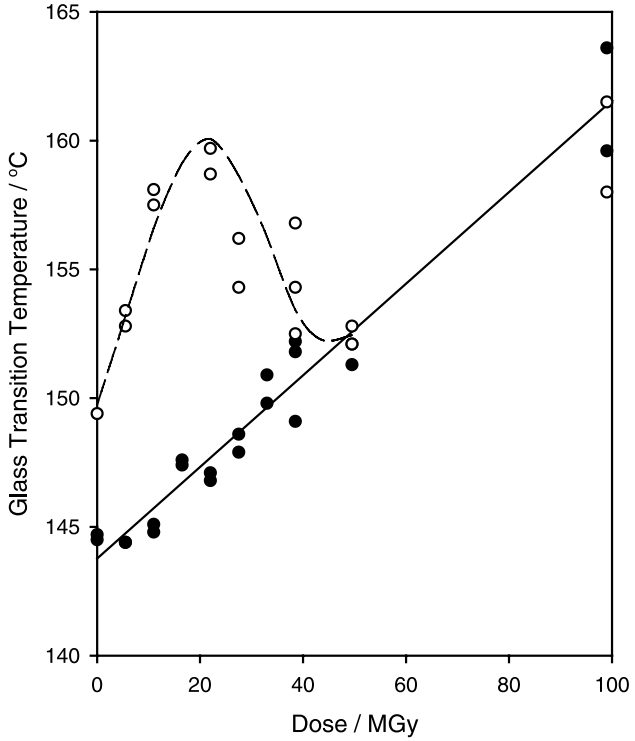

Fig. 1. Plots of glass transition temperature against radiation dose: first scan (●: solid line), second scan (○: dashed line).

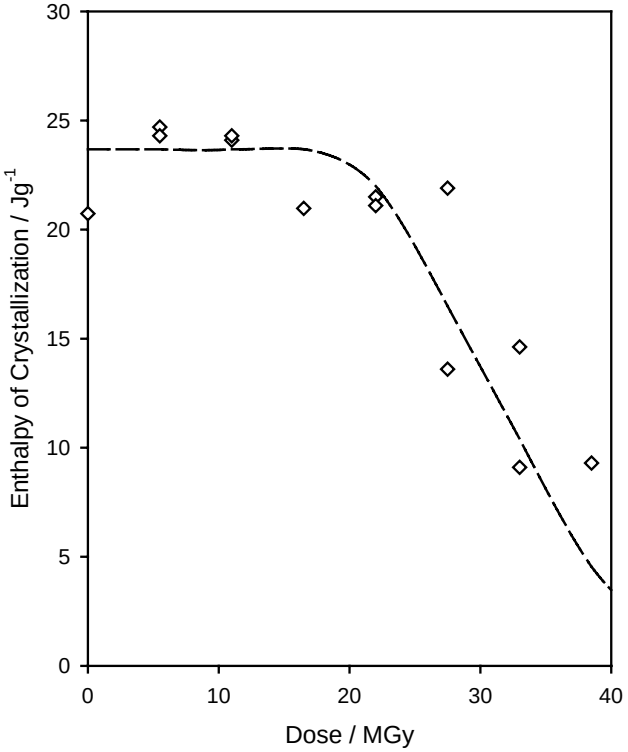

Fig. 2. Plot of first scan enthalpy of crystallization against radiation dose.

most of the specimens considered here crystallized to some degree. These samples were then rescanned to 400°C (second scan).

3. Results and discussion

The variation in observed glass transition with absorbed dose is shown in Fig. 1, for both first and second scans. Considering the first scan data (solid circles), it is evident that the glass transition temperature increases linearly with dose, D, within the range 0–100 MGy: we will subsequently represent this quantity by $T_{g1}(D)$. This linearity suggests that irradiation within this dose regime results in a linear increase in crosslink density.

The open circles in Fig. 1 indicate the dose-dependent glass transition temperatures data obtained from each specimen on rescanning: that is, after completion of one cold crystallization/melting/recrystallization cycle. We will subsequently refer to these data as $T_{g2}(D)$. Above about 50 MGy, first scan and second scan data are equivalent.

$$T_{g2}(D) = T_{g1}(D) \quad (1)$$

Such doses have, previously, been shown to prevent crystallization of amorphous PEEK on heating to above T_g [8,12] and, consequently, these data merely indicate that heating to 400°C does not result in further crosslinking via, for example, the reaction of trapped radicals, or thermal routes [13]. At lower doses, a degree of crystallization occurs above T_g, as shown in Fig. 2. Here the magnitude of the first scan crystallization exotherm is shown as a function of dose. From this it evident that, up to ~20 MGy, crystallization results in the development of an approximately constant lamellar fraction; this equates to about 18% of the system, assuming a value of 130 J g^{-1} for the enthalpy of crystallization of crystalline PEEK [14]. Above ~20 MGy, irradiation serves increasingly to inhibit crystal formation, such that no crystallization could be observed in the DSC at dose above 39 MGy.

The increase of $T_{g2}(D)$ over $T_{g1}(D)$ seen throughout the range 0–40 MGy is, qualitatively, not unexpected and can be related to two factors. First, as can be seen in the unirradiated sample, the presence of lamellae serves directly to restrict molecular mobility in the intervening amorphous layers, since $T_{g2}(0) > T_{g1}(0)$. Second, assuming that crosslinks are rejected from growing crystals, the presence of 18% crystallinity[1] will necessarily increase the local concentration of crosslinks within inter-lamellar amorphous regions over that which was, previously, present within the entirely amorphous system. The variation in $T_{g2}(D)$ with dose that can be seen in Fig. 1 can therefore be explained qualitatively by a combination of these two factors. Up to about 20 MGy, from Fig. 2, the level of crystallinity that is

[1] This figure for crystallinity is derived directly from the enthalpy of crystallization and, as such, is strictly the percentage by mass. However, the value is not greatly changed if differences between amorphous and crystalline specific volumes are taken into account.

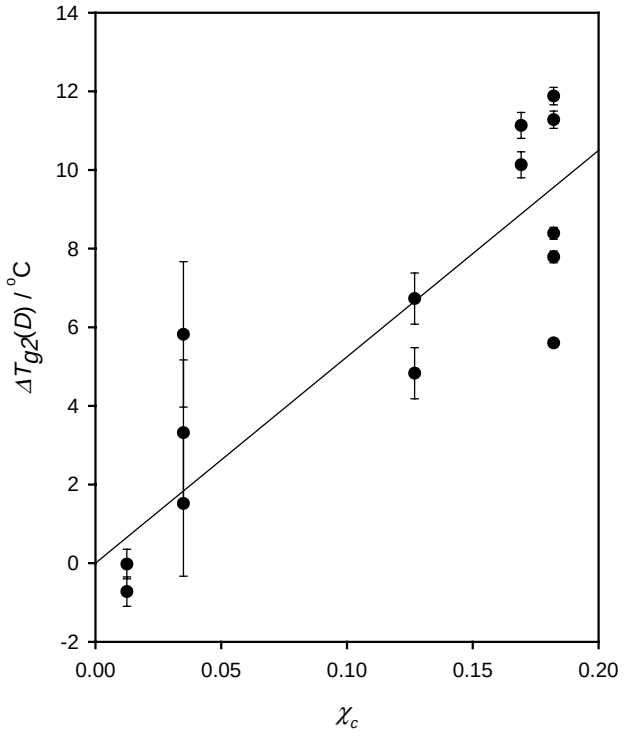

Fig. 3. Plot of excess glass transition temperature against fractional crystallinity derived from all the partially crystalline materials considered here.

able to form remains approximately constant and, consequently, the observed increase in $T_{g2}(D)$ with dose can be associated with the molecular constraints associated with accommodating increased numbers of crosslinks into the residual amorphous fraction. At a given dose, the extent of the increase of $T_{g2}(D)$ over $T_{g1}(D)$, is then dependent upon the degree of crystallinity that is able to form during the initial scan cycle. That is, the reduced amorphous volume. Up to 20 MGy, the need to accommodate more and more crosslinks into a constant amorphous volume results in $T_{g2}(D)$ increasing with D. At higher doses, this effect is more than offset by the reducing degree of crystallinity, such that the value of $T_{g2}(D)$ drops towards $T_{g1}(D)$.

The glass transition temperature of a polymer will depend upon the constraints imposed upon the amorphous phase. These will include crosslinking [9–11], crystallinity [15] and other factors which influence the local mobility, free volume and molecular packing [16,17], such as deformation, the presence of plasticizers and physical ageing. These final factors are incompatible with our experiments and, consequently, a description based upon crosslinking and crystal formation is, qualitatively, very reasonable here. However, a more quantitative analysis raises problems. From Fig. 1:

$$T_{g1}(D) = 143.8 + 0.18D \tag{2}$$

Eq. (2) relates the number of crosslinks per unit volume of amorphous material to the consequent elevation in T_g. What is now the effect of crystallization? In the simplest case, the resulting amorphous fraction would be expected to have its local crosslink density increased by a factor of $[1/(1-\chi_c)]$, where χ_c represents the volume fraction of crystals in the system. From the enthalpy data described above:

$$T_{g2}(D) = T_{g2}(0) + m_1 \frac{1}{1-\chi_c} D \tag{3a}$$

such that, initially, we would expect:

$$T_{g2}(D) = T_{g2}(0) + 0.22D \tag{3b}$$

Taking the initial linear portion of the $T_{g2}(D)$ data in Fig. 1, between 0 and 11 MGy:

$$T_{g2}(D) = 149.1 + 0.78D \tag{3c}$$

That is, the initial gradient in the $T_{g2}(D)$ data in Fig. 1 is much steeper, by almost a factor of 4, than would be expected simply on the basis of the exclusion of crosslinks from crystalline regions. Additional factors, beyond the direct effect of the crystals, that is $T_{g2}(0) > T_{g1}(0)$, and the consequent reduction in the amorphous volume, must therefore also be considered. To explore this, we have developed two models.

3.1. Crystallinity constraint model

As described above the glass transition temperature of the unirradiated partially crystalline specimen exceeds that of the equivalent amorphous material. From the amorphous perspective, we could therefore consider the crystals to behave as additional constrains, which result in what may be termed the observed excess glass transition temperature. We shall consider this effect to result from an array of effective crystalline network nodes. This excess glass transition temperature, $\Delta T_{g2}(D)$, at any dose is then simply the difference between the experimentally measured $T_{g2}(D)$ and that which would be expected if all the entanglements, radiation induced crosslinks etc were simply confined within the residual amorphous faction. That is:

$$\Delta T_{g2}(D) = T_{g2}(D) - \left[T_{g1}(0) - m_1 \frac{1}{1-\chi_c} D \right] \tag{4}$$

If this is the correct interpretation of $\Delta T_{g2}(D)$, then this should be related simply to the crystallinity of the system, at all doses. Fig. 3 shows a plot of $\Delta T_{g2}(D)$ against χ_c, where the latter parameter is derived from the dashed line in Fig. 2, and the error bars in the former are estimated from the variability seen in the measured glass transition temperature at each dose. Assuming a linear relationship between the number of effective crystalline network nodes and the crystal faction, in the range 0–20% crystallinity, the resulting correlation coefficient of 0.74 suggests that there is either considerable uncertainty in the data, which is certainly true in the low χ_c range, or that the assumed linear dependence between crystallinity and constraint is inappropriate. Indeed, this approach does not enable the form of the

experimental $T_{g2}(D)$ data in Fig. 1 to be reproduced. However, statistically, from Fig. 3, there is only about a 1% probability of $\Delta T_{g2}(D)$ and χ_c being completely uncorrelated. Crystallinity is therefore at the route of the effects seen but, equally, Fig. 3 indicates that a model based solely upon fractional crystallinity is insufficient. Consequently, we have also considered the impact of structural dimensions on T_g.

3.2. Dimensional constraint model

It has been suggested by Jonas et al. [18] that the glass transition of the amorphous component of PEEK is inversely related to its dimensions. Assuming the most simple two phase model of lamellar crystals separated by amorphous regions, then:

$$\chi_c = \frac{l_c}{l_a + l_c} \tag{5a}$$

and

$$l_a = (1 - \chi_c)(l_a + l_c) \tag{5b}$$

where l_a and l_c are the amorphous and crystalline layer thicknesses, respectively. Kalika et al. [19] investigated the relationship between l_a and T_g in PEEK using samples prepared in a variety of ways and, for values of l_a ranging from 4 to 11 nm, T_g was found to decrease linearly with increasing l_a. Whilst such a dependence may well hold over a relatively narrow l_a range, clearly, it cannot be extended to include samples which contain few crystallites: i.e. where l_a is very large. To include such materials, an alternative relationship must be devised, which should, ideally, reflect the linearly decreasing dependence of T_g with increasing l_a at small l_a values, whilst tending towards T_g for a purely amorphous PEEK sample as $l_a \rightarrow \infty$. Eq. (6) below has the necessary attributes, which is the only reason for its selection.

$$T_g = T_g(0) - \left[\frac{l_a}{l_a + K}\right][T_g(0) - T_g(\infty)] \tag{6}$$

In this, K is an arbitrary constant such that, as $l_a \rightarrow 0$, $T_g \rightarrow T_g(0)$ (T_g for amorphous material fully constrained by crystallinity) and, as $l_a \rightarrow \infty$, $T_g \rightarrow T_g(\infty)$ (T_g for amorphous material in the complete absence of crystallinity). Eliminating l_a from Eqs. (5a)–(6) and replacing the constants K, $T_g(0)$ and $T_g(\infty)$ with values derived from the data in Table 1, the glass transition temperature in unirradiated PEEK, $T_g(l_c, \chi_c)$ in degrees Celsius, can be related empirically to both the fractional crystallinity, χ_c, and the crystal thickness, l_c in nanometers, as follows:

$$T_g(l_c, \chi_c) = 180 - \frac{37 l_c(1 - \chi_c)}{3.3\chi_c + l_c(1 - \chi_c)} \tag{7}$$

This relationship could be refined by treating all the included numerical constants as additional fitable parameters. We have not attempted to do this here: rather, the indicated values were chosen simply to be consistent with available relevant data. Finally, by combining Eqs. (4) and (7) to incorporate the additional constraints that result from the accumulation of crosslinks in the amorphous phase:

$$T_{g2}(D) = 180 - \frac{37 l_c(1 - \chi_c)}{3.3\chi_c + l_c(1 - \chi_c)} + m_1 \frac{1}{1 - \chi_c} D \tag{8}$$

The dashed line in Fig. 1 was obtained using this equation: by including both crystallinty and crystal thickness, we have quantitatively reproduced our experimental $T_{g2}(D)$ data.

Table 1
Values of l_a and T_g used to estimate the parameters K, $T_g(0)$ and $T_g(\infty)$ used in Eq. (7)

l_a (nm)	T_g (°C)	Source
0	180	Ref. [16]
11.5	150	Ref. [16]
∞	143	Fig. 1

The values for the two independent parameters, crystalline fraction, χ_c, and crystal thickness, l_c, used to generate the dashed line in Fig. 1 are shown in Fig. 4. Whilst resulting agreement with the experimental $T_{g2}(D)$ data is good, are the values shown in Fig. 4 reasonable? The indicated χ_c values are equivalent to the data in Fig. 2, where they are represented by the dashed line. That is, we are assuming similar crystal fractions develop rapidly during the first heating scan and during rapid cooling in the DSC. Whilst these two processes will not be exactly equivalent, the overall degree of crystallinity that forms in PEEK is generally low [14,20,21], particularly when crystallization occurs quickly. We therefore believe that the values chosen are entirely reasonable. The apparent variation in l_c is more intriguing.

We are unaware of any direct measurements relating to crystalline development in irradiated PEEK and, therefore, any discussion of these data must be derived from indirect evidence. Blundell and Osborn [14] used X-ray scattering to investigate the effect of crystallization temperature on both the crystallinity and crystal thickness of PEEK. They reported values for these parameters that ranged from 19% and 2 nm, for cold crystallization at 200°C, to 40% and 5.9 nm for isothermal crystallization from the melt at 320°C. Lee et al. [21] and Ivanov et al. [22] have reported similar figures. In absolute terms, the data in Fig. 3 are therefore comparable with experimental results. Indeed, the highest l_c value of 3.3 nm at $D = 0$ MGy corresponds to a melt crystallization temperature of about 270°C [14,21]. Although this value is somewhat high, it does correspond to the lowest isothermal melt crystallization temperature accessed by Bassett et al. [23]. Thereafter, the monotonic decrease in l_c with dose can be related to two kinetic factors.

First, crosslinking inhibits crystal formation [8], such that crystallization during cooling in the DSC would occur at lower temperatures, so leading directly to reduced lamellar

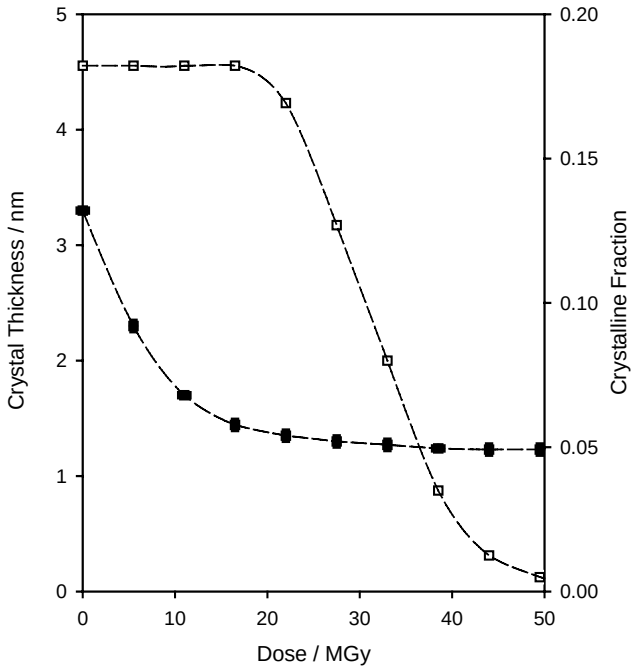

Fig. 4. Values of crystal thickness (■) and crystalline fraction (□) used in conjunction with Eq. (8) to model the second scan dose dependent glass transition data shown in Fig. 1.

thicknesses. In addition, time dependent small angle X-ray scattering studies of the annealing behaviour of PEEK suggest that, when crystals of PEEK are surrounded by poorly constrained amorphous conformations, appreciable thickening is possible [22]. Indeed, Hsiao et al. [24] have argued that cold crystallized PEEK can contain a broad population of lamellar thicknesses, which would certainly indicate a wide range of stability. Time-resolved studies of crystallization also indicate that the long period falls significantly during the early stages of the process [24,25], as a result of dominant/subsidiary crystallization. That is, dominant lamellae form first and, as a result, the long period is large. Subsequently, subsidiary lamellae develop within the existing dominant framework and, consequently, the observed long period falls. We therefore propose that, after irradiation, crystals similarly form within the network but, now, reject the crosslinks, which consequently accumulate in amorphous regions and at lamellar surfaces. Molecular relaxation studies indicate particular changes in these latter regions [26]. The extent to which dominant lamellae are able to thicken will therefore be reduced by the crosslink density at their basal planes; subsidiary crystallization may, nevertheless, occur within the remaining interstitial regions, to an extent determined by the local defect concentration. As a result, crystal thickness may be reduced after irradiation and will tend towards the thickness of the initial nuclei.

Whilst the above analysis of crystallization parameters is somewhat speculative at this point, it does explain the observations and relies upon nothing more controversial than the concept of reduced lamellar growth rates and reduced isothermal thickening when crystal formation occurs from a crosslinked melt. Thereafter, the dependence of T_g on dose is simple determined by a combination of crosslink density and the additional constraints imposed by neighbouring lamellae.

4. Conclusions

The effect of electron irradiation on the glass transition temperature of PEEK has been studied up to 100 MGy. In amorphous samples, T_g increases linearly with radiation dose, suggesting that the crosslink density similarly increases linearly within this dose range. Up to ~50 MGy, crystallization occurs above T_g. The presence of these crystallites serves to impose further constraints upon the residual amorphous fraction, which, consequently, exhibits increased T_g values. This behaviour has been explained by invoking a combination of rejection of crosslinks to dimensionally constrained amorphous regions and to lamellar surfaces, which consequently, modifies crystallite development. Quantitatively, the observed variations in T_g could only be explained through the development of a model which explicitly includes both overall crystallinity and crystal thickness.

References

[1] Yoda O. Polym Commun 1985;26(1):16–19.
[2] Sasuga T, Hagiwara M. Polymer 1987;28(11):1915–21.
[3] Connell JW, Siochi EJ, Croall CI. High Perform Polym 1993;5(1):1–14.
[4] Sasuga T, Kudoh H. Polymer 2000;41(1):185–94.
[5] Kumar S, Adams WW. Polymer 1990;31(1):15–19.
[6] Vaughan AS, Sutton SJ. Polymer 1995;36(8):1549–54.
[7] Sasuga T, Hagiwara M. Polymer 1985;26(4):501–5.
[8] Vaughan AS, Stevens GC. Polymer 1995;36(8):1531–40.
[9] Fox TG, Loshaek S. J Polym Sci 1955;15(80):371–90.
[10] Stejny J. Polym Bull 1996;36(15):617–21.
[11] Ueberreiter K, Kanig G. J Chem Phys 1950;18(4):399–406.
[12] Yoda O. Polym Commun 1984;25(8):238–40.
[13] Zhang Z, Zeng H. Polymer 1993;34(17):3648–52.
[14] Blundell DJ, Osborn BN. Polymer 1983;24(8):953–8.
[15] Wu Z, Zheng YB, Yu HX, Seki M, Yosomiya R. Die Angew Makromol Chem 1988;164(2645):21–34.
[16] Gomez Ribelles JL, Diaz-Calleja R, Ferguson R, Cowie JMG. Polymer 1987;28(13):2262–6.
[17] McKenna GB. In: Allen G, Bevington JC, Booth C, Price C, editors. Comprehensive polymer science, vol. 1. Oxford: Pergamon Press, 1989. p. 311–62.
[18] Jonas A, Legras R, Issi J-P. Polymer 1991;32(18):3364–70.
[19] Kalika DS, Gibson DG, Quiram DJ, Register RA. J Polym Sci, Part B: Polym Phys 1998;36(1):65–73.
[20] Chang S-S. Polym Commun 1988;29(5):138–41.
[21] Lee Y, Porter RS, Lin JS. Macromolecules 1989;22(4):1756–60.
[22] Ivanov DA, Legras R, Jonas AM. Polymer 2000;41(10):3719–27.
[23] Bassett DC, Olley RH, Al Raheil IAM. Polymer 1988;29(10):1745–54.
[24] Hsiao BS, Gardner KH, Wu DQ, Chu B. Polymer 1993;34(19):3996–4003.
[25] Wang J, Alvarez M, Zhang W, Wu Z, Li Y, Chu B. Macromolecules 1992;25(25):6943–51.
[26] Sasuga T, Hagiwara M. Polymer 1986;27(6):821–6.